

J/ψ production associated with a W -boson at the 7 TeV LHC

Song Mao^a, Li Gang^a, Ma Wen-Gan^b, Zhang Ren-You^b, Guo Lei^b, and Guo Jian-You^a

^a School of Physics and Material Science, Anhui University, Hefei, Anhui 230039, P.R.China

^b Department of Modern Physics, University of Science and Technology of China (USTC),
Hefei, Anhui 230026, P.R.China

Abstract

We calculate the complete next-to-leading order (NLO) QCD corrections to the $J/\psi + W$ associated production within the factorization formalism of nonrelativistic QCD at the 7 TeV LHC. We provide the numerical results for the leading-order (LO), NLO QCD corrected differential cross sections of the J/ψ transverse momentum by adopting the event selection criteria requested by the ATLAS experiment. We find that the differential cross section at the LO is significantly enhanced by the NLO QCD corrections.

PACS: 12.38.Bx, 12.39.St, 14.60.Lc

Recently, after we published our work on the QCD corrections to J/ψ production in association with a W -boson at the 14 TeV LHC [1], Darren Price in the ATLAS experiment suggested us to extend our study to the colliding energy of 7 TeV , and asked for theoretical predictions for the corresponding differential cross sections in the restricted kinematic regions of the final particles. In Ref.[1] we presented the detailed calculations of the NLO QCD corrections to the $J/\psi + W$ associated production at the $\sqrt{s} = 14 TeV$ LHC, but not for the 7 TeV LHC. In this letter, we calculate the NLO QCD corrections to the associated J/ψ production with a W gauge boson in the nonrelativistic QCD (NRQCD) at the 7 TeV LHC, and provide the theoretical predictions for the p_T distribution of J/ψ by adopting the event selection criteria requested by the ATLAS experiment.

We calculate the $pp \rightarrow J/\psi + W + X$ process by applying the covariant-projector method [2] in the NRQCD framework. Some representative Feynman diagrams for the partonic process $u\bar{d} \rightarrow J/\psi + W^+$ at the LO and the QCD NLO are depicted in Fig.1. The cross section for the $pp \rightarrow J/\psi + W + X$ process is expressed as

$$\begin{aligned} \sigma(pp \rightarrow J/\psi + W + X) &= \sum_{(ij),n} \int dx_1 dx_2 \frac{\langle \mathcal{O}^H[n] \rangle}{N_{col}(n)N_{pol}(n)} \hat{\sigma}(i + j \rightarrow c\bar{c}[n] + W, \hat{s} = x_1 x_2 s) \\ &\times [G_{i/A}(x_1, \mu_f) G_{j/B}(x_2, \mu_f) + (A \leftrightarrow B)], \end{aligned} \quad (0.1)$$

where $(ij) = (u\bar{d})$ and $(\bar{u}d)$, $N_{col}(n)$ and $N_{pol}(n)$ refer to the numbers of colors and polarization of $c\bar{c}[n]$ states produced [2], respectively. $\hat{\sigma}$ is the cross section for the short distance production of a $c\bar{c}$ quark pair in the color, spin and angular momentum state n at the parton level. $\langle \mathcal{O}^{J/\psi}[n] \rangle$ is the long distance matrix element, which describes the hadronization of the $c\bar{c}$ quark pair into the observable charmonium state J/ψ . $G_{i,j/A,B}$ are the parton distribution functions (PDFs), A and B refer to incoming protons at the LHC. We ignore the processes which are suppressed by a tiny Kobayashi-Maskawa factor.

In the leading order (LO) calculations, only the Fock state $^3S_1^{(8)}$ is involved. However, for the NLO QCD corrections to this process, we need to consider both the virtual corrections and the real gluon/light-quark emission processes. The virtual corrections only contain the contribution from $c\bar{c}$ Fock state $^3S_1^{(8)}$, while the real gluon/light-quark emission processes should involve $^1S_0^{(8)}$, $^3S_1^{(8)}$ and $^3P_J^{(8)}$ Fock states. In our calculations, we apply the dimensional regularization (DR) scheme to regularize the UV and IR divergences, and the modified minimal subtraction ($\overline{\text{MS}}$) and on-mass-shell

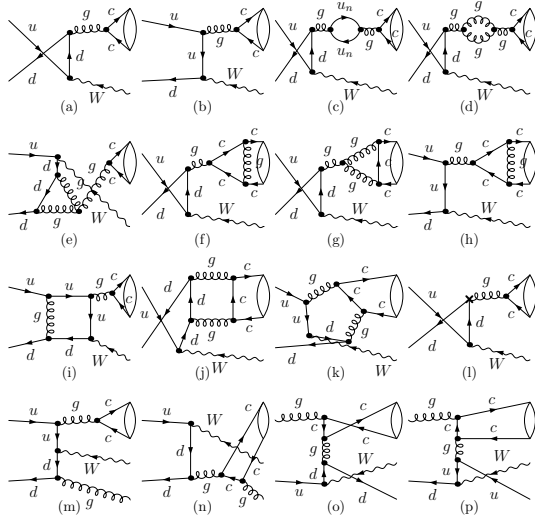


Figure 1: Representative Feynman diagrams for the partonic process $u\bar{d} \rightarrow J/\psi + W^+$ at the LO and the QCD NLO.

schemes to renormalize the strong coupling constant and the quark wave functions, respectively. In Fig.2, we present the divergence structure and divergence cancellation routes in the NLO calculation for the $pp \rightarrow J/\psi + W^+ + X$ process. In the virtual correction calculations, we find that only Fig.1(f) and Fig.1(h) induce Coulomb singularities, and we use a small relative velocity v between c and \bar{c} to regularize them [3]. The two cutoff phase space slicing method (TCPSS)[4] has been employed for dealing with the soft and collinear singularities in real gluon/light-quark emission corrections.

We take CTEQ6L1 PDFs with the one-loop running α_s in the LO calculations and CTEQ6M PDFs with the two-loop α_s in the NLO calculations [5], respectively. For simplicity we define $\mu \equiv \mu_r = \mu_f$ and take the renormalization/factorization and NRQCD scales as $\mu = m_T^{J/\psi}$ or m_W , $\mu_\Lambda = m_c$, respectively, where $m_T^{J/\psi} = \sqrt{(p_T^{J/\psi})^2 + m_{J/\psi}^2}$ is the J/ψ transverse mass. The masses of the external particles and the fine structure constant are taken as $m_W = 80.398$ GeV, $m_c = \frac{1}{2}m_{J/\psi} = 1.5$ GeV and $\alpha = 1/137.036$. We use two sets of color-octet (CO) long distance matrix elements (LDME) listed in Table 1 as the input parameters, which were obtained by fitting the differential cross section and polarization of inclusive J/ψ production data from various experiments [6, 7].

We calculate the LO and NLO QCD corrected cross sections for the $pp \rightarrow J/\psi + W \rightarrow J/\psi + \mu + \nu_\mu + X$ process at the 7 TeV LHC by adopting the following kinematic cuts on the final particles

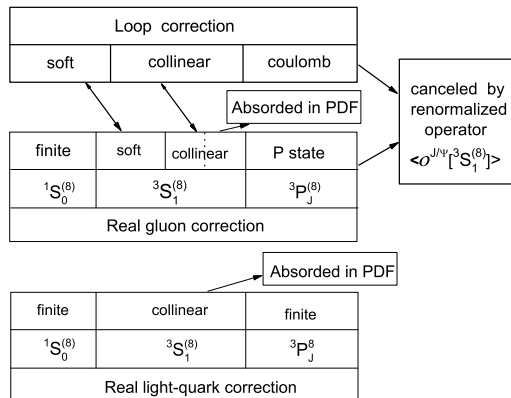


Figure 2: The divergence structure and divergence cancellation routes in the NLO calculations for the $pp \rightarrow J/\psi + W^+ + X$ process.

	Set 1 (GeV^3)	Set 2 (GeV^3)
$\langle \mathcal{O}^{J/\psi}[^1S_0^{(8)}] \rangle$	3.04×10^{-2}	8.9×10^{-2}
$\langle \mathcal{O}^{J/\psi}[^3S_1^{(8)}] \rangle$	1.68×10^{-3}	3×10^{-3}
$\langle \mathcal{O}^{J/\psi}[^3P_0^{(8)}] \rangle$	-9.08×10^{-3}	5.6×10^{-3}

Table 1: Two sets of CO LDME for J/ψ . Set 1 are extracted via a global fit from various hadroproduction, photoproduction, two-photon scattering and electron-positron annihilation experiments [6]. Set 2 are extracted by fitting the differential cross section and polarization of prompt J/ψ simultaneously at the Tevatron [7].

according to the requests of the ATLAS data analyses:

$$p_T^\mu > 25 \text{ GeV}, \quad |\eta^\mu| < 2.4, \quad p_T^\nu > 20 \text{ GeV}, \quad m_T^W > 40 \text{ GeV}. \quad (0.2)$$

where m_T^W is W boson transverse mass defined as $m_T^W = \sqrt{2p_T^\mu p_T^\nu [1 - \cos(\phi^\mu - \phi^\nu)]}$, and $\phi^\mu - \phi^\nu$ is the angle between muon and neutrino in the transverse plane [8].

In our calculations the uncertainty for theoretical prediction mainly comes from two parts: the short distance part and the long distance part. For the former part, the dependence of the cross section on the renormalization scale μ_r and factorization scale μ_f induces theoretical uncertainty. For the later part, the values of CO LDME for the J/ψ extracted from the experiments by different experimental groups vary significantly. In the following tables and figures, we will give the results by adopting two set of CO LDME and two typical scales ($\mu = m_T^{J/\psi}, m_W$).

In Table 2 and Table 3, we provide the cross sections for the $pp \rightarrow J/\psi + W \rightarrow J/\psi + \mu + \nu_\mu + X$ process at the 7 TeV LHC in the $p_T^{J/\psi}$ and the J/ψ rapidity intervals by taking the two different

$p_T^{J/\psi}$ [GeV]	$\mu = m_T^{J/\psi}$				$\mu = M_W$			
	$ y_{J/\psi} < 1.0$		$1.0 < y_{J/\psi} < 2.1$		$ y_{J/\psi} < 1.0$		$1.0 < y_{J/\psi} < 2.1$	
	LO [fb]	NLO [fb]	LO [fb]	NLO [fb]	LO [fb]	NLO [fb]	LO [fb]	NLO [fb]
8.5~10	0.567	2.96	0.531	2.87	0.361	1.75	0.336	1.45
10~14	0.960	4.86	0.899	4.65	0.637	3.10	0.593	2.52
14~18	0.527	2.56	0.494	2.42	0.369	1.81	0.344	1.45
18~22	0.315	1.51	0.296	1.40	0.230	1.14	0.215	0.896
22~30	0.331	1.54	0.311	1.44	0.253	1.27	0.238	0.990

Table 2: The cross sections for the $pp \rightarrow J/\psi + W \rightarrow J/\psi + \mu + \nu_\mu + X$ process at the 7 TeV LHC in the $p_T^{J/\psi}$ and the J/ψ rapidity intervals by taking the Set 1 LDME parameters.

$p_T^{J/\psi}$ [GeV]	$\mu = m_T^{J/\psi}$				$\mu = M_W$			
	$ y_{J/\psi} < 1.0$		$1.0 < y_{J/\psi} < 2.1$		$ y_{J/\psi} < 1.0$		$1.0 < y_{J/\psi} < 2.1$	
	LO [fb]	NLO [fb]	LO [fb]	NLO [fb]	LO [fb]	NLO [fb]	LO [fb]	NLO [fb]
8.5~10	1.01	3.51	0.949	3.66	0.645	2.58	0.600	1.91
10~14	1.71	5.64	1.60	5.69	1.14	4.54	1.06	3.19
14~18	0.942	2.91	0.883	2.82	0.659	2.61	0.615	1.77
18~22	0.562	1.67	0.528	1.59	0.410	1.62	0.384	1.06
22~30	0.591	1.67	0.555	1.57	0.452	1.80	0.424	1.13

Table 3: The cross sections for the $pp \rightarrow J/\psi + W \rightarrow J/\psi + \mu + \nu_\mu + X$ process at the 7 TeV LHC in the $p_T^{J/\psi}$ and the J/ψ rapidity intervals by taking the Set 2 LDME parameters.

set of LDME parameters. In each table, we list the differential cross sections for $\mu_r = \mu_f = m_T^{J/\psi}$ and $\mu_r = \mu_f = m_W$, respectively. We adopt the event select criteria with the cuts of $p_T^\mu > 25 \text{ GeV}$, $|\eta^\mu| < 2.4$, $p_T^{\text{miss}} > 20 \text{ GeV}$ and $m_T^W > 40 \text{ GeV}$ as requested by ATLAS experiment where muon and neutrino are the W decay products. In these two tables we list the J/ψ production rates in the following $p_T^{J/\psi}$ intervals of 8.5 ~ 10 GeV, 10 ~ 14 GeV, 14 ~ 18 GeV, 18 ~ 22 GeV, 22 ~ 30 GeV, and the J/ψ rapidity intervals of $|y_{J/\psi}| < 1.0$ and $1.0 < |y_{J/\psi}| < 2.1$, separately. The cross section for the $pp \rightarrow J/\psi + W \rightarrow J/\psi + \mu + \nu_\mu + X$ process is obtained via the cross section for $pp \rightarrow J/\psi + W + X$ multiplying the branching fraction for the $W \rightarrow \mu\nu_\mu$ decay, which is taken as 10.57% [9].

In Figs.3(a,b) and Figs.4(a,b), we present the the LO and NLO QCD corrected distributions of the transverse momentum of J/ψ for the $pp \rightarrow J/\psi + W \rightarrow J/\psi + \mu + \nu_\mu + X$ process at the 7 TeV LHC in the region restricted by the conditions shown in (0.2) by adopting the Set 1 LDME parameters. The renormalization/factorization scales are set to be $\mu = m_T^{J/\psi}$ and $\mu = m_W$ in Figs.3 and Figs.4, separately. In Figs.3(a,b) and Figs.4(a,b), we give the predictions for the transverse momentum

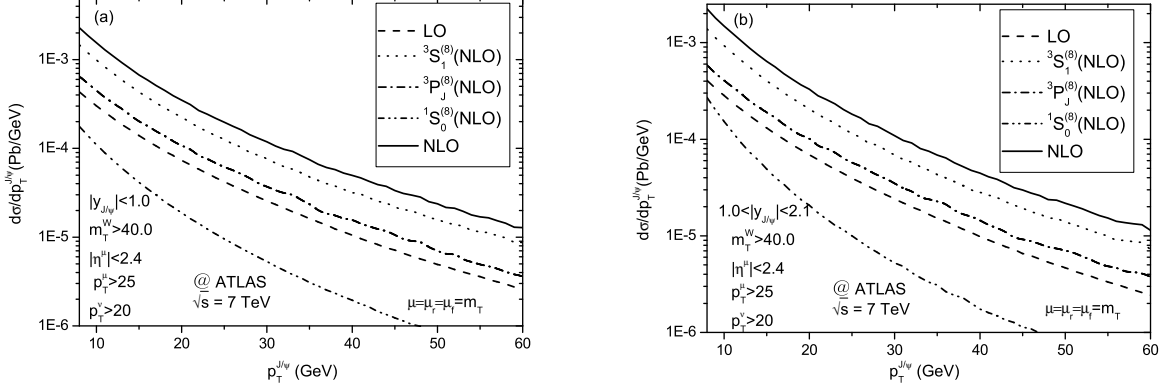


Figure 3: The LO and NLO QCD corrected distributions of the transverse momentum of J/ψ for the $pp \rightarrow J/\psi + W \rightarrow J/\psi + \mu + \nu_\mu + X$ process at the 7 TeV LHC in the region with the constraints on final particles shown in (0.2) by taking the Set 1 LDME parameters and $\mu = \mu_r = \mu_f = m_T^{J/\psi}$. (a) $|y_{J/\psi}| < 1.0$, (b) $1.0 < |y_{J/\psi}| < 2.1$.

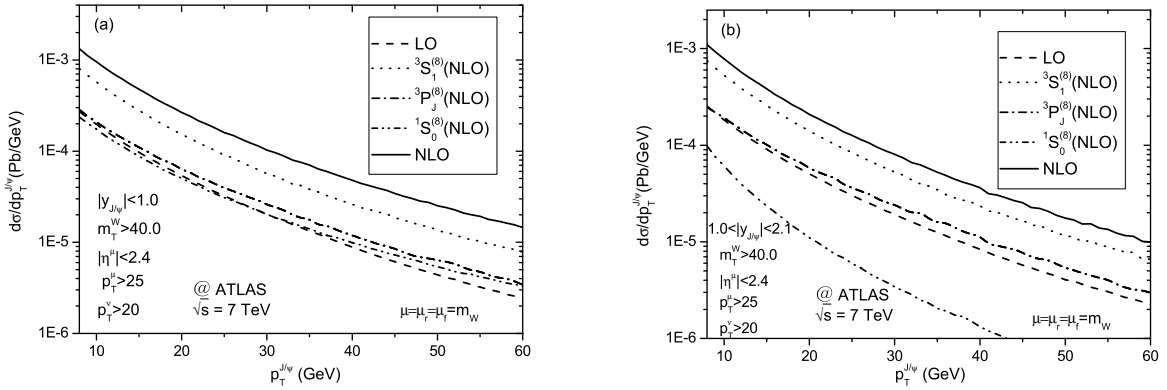


Figure 4: The LO and NLO QCD corrected distributions of the transverse momentum of J/ψ for the $pp \rightarrow J/\psi + W \rightarrow J/\psi + \mu + \nu_\mu + X$ process at the 7 TeV LHC in the region with the constraints on final particles shown in (0.2) by taking the Set 1 LDME parameters and $\mu = \mu_r = \mu_f = m_W$. (a) $|y_{J/\psi}| < 1.0$, (b) $1.0 < |y_{J/\psi}| < 2.1$.

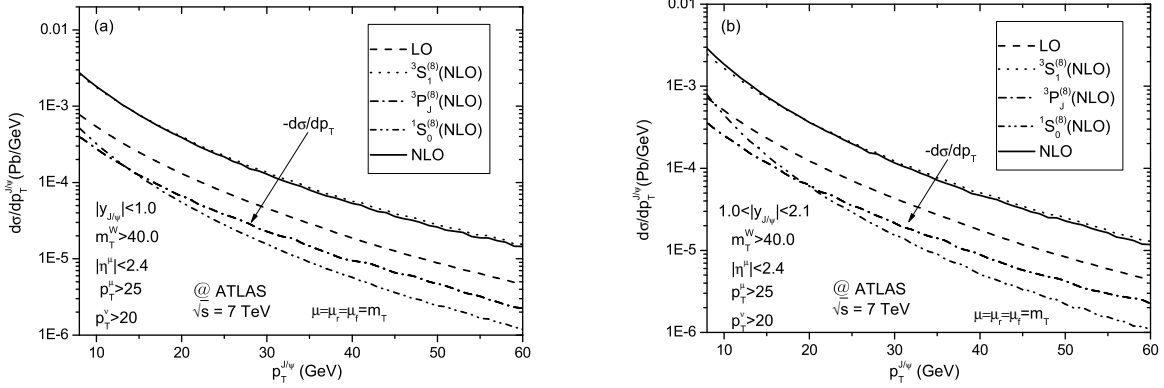


Figure 5: The LO and NLO QCD corrected distributions of the transverse momentum of J/ψ for the $pp \rightarrow J/\psi + W \rightarrow J/\psi + \mu + \nu_\mu + X$ process at the 7 TeV LHC in the region with the constraints on final particles shown in (0.2) by taking the Set 2 LDME parameters and $\mu = \mu_r = \mu_f = m_T^{J/\psi}$. (a) $|y_{J/\psi}| < 1.0$, (b) $1.0 < |y_{J/\psi}| < 2.1$.

distributions of J/ψ in two rapidity intervals on the J/ψ : $|y_{J/\psi}| < 1.0$ and $1.0 < |y_{J/\psi}| < 2.1$. As a comparison, we also depict the contributions from the $^1S_0^{(8)}$ and $^3S_1^{(8)}$ and $^3P_J^{(8)}$ Fock states in Figs.3(a,b) and Figs.4(a,b). The short distance part of the differential cross section contributed by the $^3P_J^{(8)}$ ($J = 0, 1, 2$) Fock states is negative, and the LDME $\langle \mathcal{O}^{J/\psi}[^3P_0^{(8)}] \rangle$ with Set 1 LDME parameters is also negative. We can see from Eq.(0.1) that the differential cross section contributed by the $^3P_J^{(8)}$ ($J = 0, 1, 2$) Fock states should be positive. These figures show clearly that the differential cross section at the LO is significantly enhanced by the QCD corrections.

In Figs.5(a,b) and Figs.6(a,b), we give the LO and NLO QCD corrected distributions of the transverse momentum of J/ψ for the $pp \rightarrow J/\psi + W \rightarrow J/\psi + \mu + \nu_\mu + X$ process at the 7 TeV LHC taking the Set 2 LDME parameters in the region restricted by the fiducial cuts on final particles as shown in (0.2). The renormalization/factorization scales are set to be $\mu = m_T^{J/\psi}$ and $\mu = m_W$ in Figs.5(a,b) and Figs.6(a,b), separately. We also give the predictions for the transverse momentum distributions of J/ψ in two J/ψ rapidity intervals: $|y_{J/\psi}| < 1.0$ and $1.0 < |y_{J/\psi}| < 2.1$. Fig.5(a), Fig.6(a) are for $|y_{J/\psi}| < 1.0$, and Fig.5(b), Fig.6(b) for $1.0 < |y_{J/\psi}| < 2.1$. The short distance contribution part from the $^3P_J^{(8)}$ ($J = 0, 1, 2$) Fock states is negative, while the LDME $\langle \mathcal{O}^{J/\psi}[^3P_0^{(8)}] \rangle$ with Set 2 LDME parameters is also positive, thus the contribution from $^3P_J^{(8)}$ ($J = 0, 1, 2$) Fock states is negative. The negative contributions of $^3P_J^{(8)}$ ($J = 0, 1, 2$) Fock states are also presented in

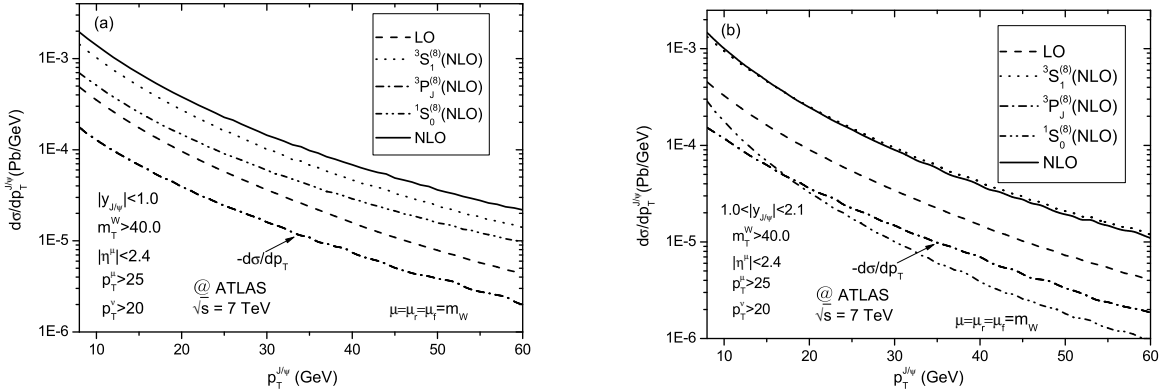


Figure 6: The LO, NLO QCD corrected distributions of the transverse momentum of J/ψ for the $pp \rightarrow J/\psi + W \rightarrow J/\psi + \mu + \nu_\mu + X$ process at the 7 TeV LHC in the region with the constraints on final particles shown in (0.2) by taking the Set 2 LDME parameters and $\mu = \mu_r = \mu_f = m_W$. (a) $|y_{J/\psi}| < 1.0$, (b) $1.0 < |y_{J/\psi}| < 2.1$.

Figs.5(a,b) and Figs.6(a,b) for comparison.

In summary, we provide the predictions on the $J/\psi + W$ associated production within the factorization formalism of the nonrelativistic QCD at the 7 TeV LHC using the parameters and kinematic constraints suggested by the ATLAS experiment. We show the distributions of the transverse momentum of J/ψ for the $pp \rightarrow J/\psi + W \rightarrow J/\psi + \mu + \nu_\mu + X$ process in a region constrained by putting the cuts on final particles shown in (0.2), and using the two set of LDME parameters and two typical energy scales separately. Our results show that the theoretical uncertainties come from the choices of the scales and the CO LDME parameters.

Acknowledgments: The authors would like thank Mr. Darren Price for helpful discussion. This work was supported in part by the National Natural Science Foundation of China (No.11205003, No.11275190, No.11075150, No.11005101, No. 11175001), the Key Research Foundation of Education Ministry of Anhui Province of China (No. KJ2012A021), the Youth Foundation of Anhui Province(No. 1308085QA07), and financed by the 211 Project of Anhui University (No.02303319).

References

- [1] G. Li, M. Song, R.Y. Zhang, and W.G. Ma, Phys. Rev. **D 83** (2011) 014001, arXiv:1012.3798.

- [2] A. Petrelli, M. Cacciari, M. Greco, F. Maltoni, M.L. Mangano, Nucl. Phys. **B 514** (1998) 245.
- [3] M. Kramer, Nucl. Phys. **B 459**, 3 (1996).
- [4] B.W. Harris and J.F. Owens, Phys. Rev. **D 65**, 094032 (2002).
- [5] J. Pumplin, D.R. Stump, J. Huston, H.L. Lai, P. Nadolsky, and W.K. Tung, JHEP **0207**, 012 (2002).
- [6] M. Butenschoen, B.A. Kniehl, Nucl. Phys. **B Proceedings Supplement XX** (2012) 1-11.
- [7] K.T. Chao, Y.Q. Ma, H.S. Shao, K. Wang, Y.J. Zhang, Phys. Rev. Lett. **108**, 242004 (2012).
- [8] The ATLAS Collaboration, 'Measurement of the cross-section for W boson production in association with b-jets in pp collisions at $\sqrt{s} = 7$ TeV with the ATLAS detector', arXiv:1302.2929.
- [9] J. Beringer et al. (Particle Data Group), Phys. Rev. **D 86**, 010001(2012).